Experimental study on liquid sloshing with dual vertical porous baffles in a sway excited tank

K.V. Sahaj[*1], T. Nasar[2] and K.G. Vijay[3]

[1]Department of Water Resources and Ocean Engineering,
National Institute of Technology Karnataka, Mangalore, India
[2]Department of Water Resources and Ocean Engineering,
National Institute of Technology Karnataka, Mangalore, India
[3]Department of Ocean Engineering, Indian Institute of Technology Madras, Chennai, India

Abstract. Sloshing behavior of liquid within containers represents one of the most fundamental fluid-structure interactions. Liquid in partially filled tanks tends to slosh when subjected to external disturbances. Sloshing is a vicious resonant fluid motion in a moving tank. To understand the effect of baffle positioned at $L/3$ and $2L/3$ location, a shake table experiments was conducted for different fill volumes of aspect ratio 0.163, 0.325 and 0.488. For a fixed amplitude of 7.5 mm, the excitation frequencies are varied between 0.457 *Hz* to 1.976 *Hz*. Wave probes have been located at both tank ends to capture the surface elevation. The experimental parameters such as sloshing oscillation and energy dissipation are discussed here. Comparison is done for with baffles and without baffles conditions. For both conditions, the results showed that aspect ratio of 0.163 gives better surface elevation and energy dissipation than obtained for aspect ratio 0.325 and 0.488. Good agreement is observed when numerical analysis is compared with the experiments results.

Keywords: energy dissipation; excitation frequencies; sloshing oscillation

1. Introduction

The appearance of fluctuations on the free surface of a tank partially filled with liquid is observed when external loads are applied. This movement's amplitude is referred to as Sloshing. External excitation, the liquid's level and physical qualities, as well as the tank's construction, all play a role. The fluid particles' free surface mobility reflects the fluid field's overall movement. The prevention of a tank's stability and resistance throughout the design phase is a critical consideration. Liquid sloshing is related to a variety of practical applications and engineering issues, such as the behavior of liquid tankers on ship bridges, the motion of liquid fuel on airlines during flight, and the seismic response of large storage liquid containers.

The sloshing force generated on the side wall of the tank is found to be reduced significantly. Sloshing is the movement of the free surface of the liquid inside the partly filled tanker in fluid dynamics. This is a common occurrence in spacecraft tanks, cargo ship fuel tanks, and trucks transporting fuels or water. Sloshing is an undesirable phenomenon which occurs in nuclear reactors

---

∗Corresponding author, Research Scholar, E-mail: sahaj30.k.v@gmail.com

during an earthquake. The intensity of sloshing of liquid inside a moving tank is influenced by a number of factors including liquid fill depth, tank geometry, liquid type, and tank motion. Oscillation of the water in the partially filled vessel due to the external force is called sloshing. Sloshing is observed in many of the engineering applications such as oil carrying ships, liquid transporting trucks and trains, space crafts and rockets, water oscillation in reservoirs and fluid storage tanks when subjected to earthquakes. Sloshing occurs when a moving tank contains a liquid with a free surface, causes significant movements and excitation forces. A partially full tank is subjected to significant liquid motions when the hosting-vessel movement includes energy around its normal sloshing frequencies. Many experiments have been undertaken to prevent strong liquid motions and minimize sloshing forces in the sloshing problem. This can be accomplished with both solid and porous baffles. Liquid sloshing has a substantial detrimental impact on highway container truck directional dynamics and safety performance. The stability limit and controllability of partially-filled tank vehicles are reduced by hydrodynamic forces and moments generated by liquid cargo oscillations in the tank during steering or braking operations.

Exporting and importing oils through the countries is the one of the main trading. Transporting oil and water are mainly through the water waters ways and land base that is truck and trains. Sloshing is severe problem in the oil carrying ship because of oscillation of the oil inside the tank and it is one of the main reason for instability and damage of the oil carrying ships. Knowing the sloshing effect will be helpful for engineers to design the oil carrying ships and transit truck tanks. There are so many experiments have been going on for solving the sloshing problems. In the late 1980's, extensive research was conducted on the phenomenon of sloshing. The predicted pressure time traces were compared to the experimental pressure movement in a roll excited tank (Akyildiz and Ünal 2005). Armenio and La Rocca (1996) used together experimental and numerical methods to investigate sloshing oscillation behavior in excited tank. In a combined sway and heave excitation Frandsen (2004) identified several resonance conditions. Kim *et al.* (2017) investigated scale effects on 3-D sloshing flows by conducting a sequence of model experiments for three tanks of varying sizes. A statistical approach was used to evaluate the primary sloshing load parameters, and the results from experiments at different scales (15 percent, 70 percent, and 95 percent) were compared. In an elastic tank, Mei-rong *et al.* (2014) analyzed the characteristics and variance of sloshing elevation and pressure. Using finite element analysis, Nakayama and Washizu (1980) investigated liquid motion and the resultant spilling density in a container subjected to forced fluctuations using a nonlinear method. Nasar *et al.* (2012) studied the wave-induced impact pressure on a normal beam sea condition in an experimental study. Xue *et.al* (2017) reported the impact of the vertical baffles on the sloshing frequency with shake table tests. A horizontal baffle close to free surface can also help to control the sloshing motion. The horizontal and vertical baffles were compared by (Isaacson and Premasiri 2001) who found that the horizontal baffle is more effective in dampening liquid sloshing motion in deeper tanks, whereas the vertical baffle is ideal for shallow tanks. Cho *et al.* (2017) demonstrated that an impervious horizontal baffle decreases the impulsive sloshing pressure on a tank ceiling using the finite-difference method. (Biswal *et al*. 2004, Goudarzi *et al*. 2012) reduced maximum sloshing wave heights that can be achieved by lowering the submergence depth or prolonging the length of horizontal baffle. According to Yu *et al.* (2019), horizontal baffles have a major dampening impact in slender tanks, while vertical baffles are more efficient in wider tanks. Various solidity ratios, slot sizes, location, and slat screen number were used to investigate screen-affected sloshing experimentally with the results indicating that sloshing reduction tends to increase as screen number increases under the experimentally specified screen locations. Nasar *et al.* (2019) conducted experiments to determine the effectiveness of porous baffles in various configurations.

Porous baffles placed at *l*/2, *l*/3, and 2*l*/3 of the tank length were found to perform better than solid submerged baffles placed at *1*/2 of the tank length. Jin *et al.* (2017) in numerical simulation, the tank with horizontal slat-type screen shows huge suppression in horizontal screen during first order sloshing but it is inadequate on third order sloshing. IL-Hyoung and Cho (2015) identified that at the resonant frequencies, the additional mass had a negative value and the damping curve had a high peak. Kang *et al.* (2019) explored while using a floating baffle to reduce sloshing in an LNG tank without trying to replace it. In the test method, the sloshing effect in a membrane style LNG tank model was induced by sway motion with 30 percent and 50 percent filling conditions. The results showed that using a floating baffle successfully reduced surface run-up and impulsive pressure. The performance of a surface fixed horizontal porous wave barrier in normal waves was investigated using experimental and computational methods (Poguluri *et al.* 2021). CFD simulations were used to recreate the qualitative wave action propagating over a horizontal porous barrier. The surface-fixed horizontal barrier was found to be more efficient in dissipating wave energy in the short wave duration field, with more energy transfer from the first harmonic to higher harmonics as porosity is increased. The present study focuses on finding out the sloshing oscillation and energy dissipation in three different fill levels in a sway excited rectangular tanks.

Experimental studies have been done here to know the sloshing effects. Sloshing impact will be more on the end walls. Knowing the sloshing effect will helpful for engineers to design the oil carrying ships and transit truck tanks. There are so many experiments have been going on to solve the sloshing problems. Anti-slosh devices, such as baffles, are usually encountered to mitigate the adverse effects of liquid slosh on tank vehicle directional performance and stability. Baffles are commonly used to reduce sloshing oscillations, especially peak oscillations, and to decrease instability by enhancing damping. The hydrodynamic forces associated with baffle arrangements must be investigated in order to build the baffle. The arrangement of baffles including number of baffles, location, size and porosity of the baffles are taken into consideration for damping. Excitation amplitude, excitation frequency, water depth in the tank, shake table motion, size and geometry of tank also affect the damping.

2. Experimental investigation

The set up for the experimental work includes a hydraulic shake table along with a digital wave form generator. Using the hydraulic actuator, the shake table is operated which is connected to a hydraulic power jack as shown in Fig. 1. The frequency and amplitude of excitation are controlled with the support of a wave transformer. Load cells of capacity with 50kgf are used to measure the sloshing forces. To measure horizontal displacement caused by the shake table and table motion LVDT of ±50 mm was used.

The partially liquid filled tank is attached on the shake table and the table is excited harmonically at the required excitation frequency. The frequencies of excitation ranged from 0.457 *Hz* to 1.976 *Hz* covering fifth mode sloshing frequencies. Within the frequency range seventeen discrete frequencies and excitation amplitude of 7.5 mm is considered.

The partially filled tank are all influenced by the amplitude and excitation frequency, container size and its geometry, fill level and configuration of the baffle used. Ibrahim (2005) showed that in a rectangular tank the linear estimate of resonant fluid sloshing frequencies (*Hz*). For the nth mode as follows
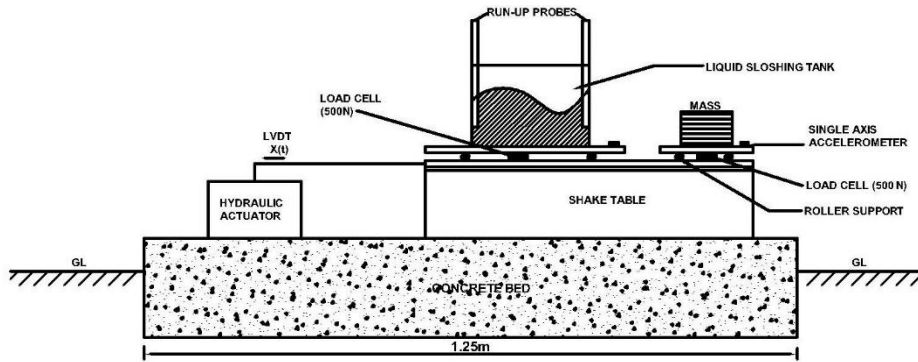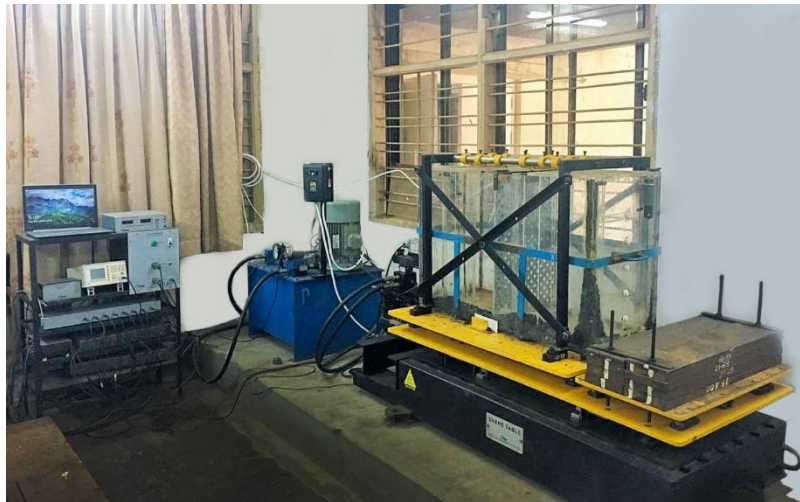
Fig. 1 Cross-section of liquid tank on shake table

Fig. 2 Photographic view of the shake table and sloshing tank

$$f_n = \frac{1}{2\pi}\sqrt{\frac{n\pi g}{L}\tanh\left(\frac{n\pi h_s}{L}\right)} \quad n=1,2,3 \qquad\qquad \ldots\ldots\ldots(1)$$

Where L is the tank length, h_S is the static liquid depth, and n is the surface mode number.

If the frequency of excitation is very nearby sloshing frequency of liquid, then the liquid sloshes with better oscillations.

3. Details of laboratory model of tank

A 1:43 scaled liquid sloshing tank (Nasar *et al.* 2012) was used in the study. The tank was fabricated using acrylic sheets of 12 mm thickness with inner dimensions of 1.0 m (l) x 0.4 m (b) x 0.65 m (h) is as shown in Fig. 3. Porous baffles made up of mild steel plate of thickness 2 mm was
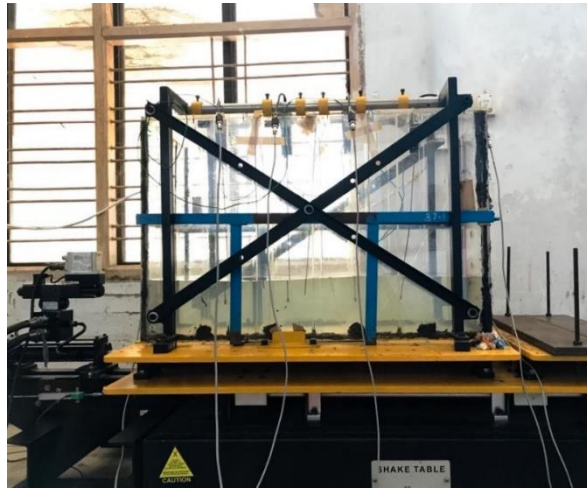
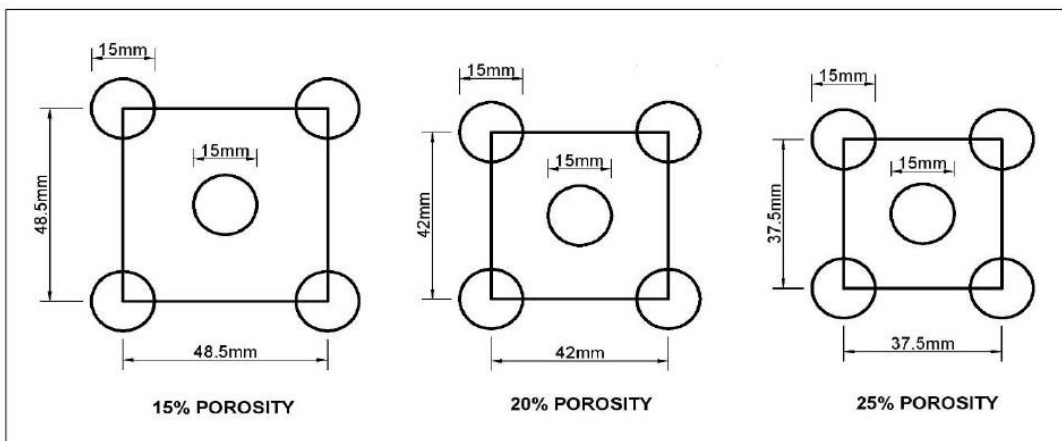Fig. 3 Photographic of liquid filled tank

Fig. 4 Size of pores in baffles wall for different staggered position of 15%, 20% and 25% porosities
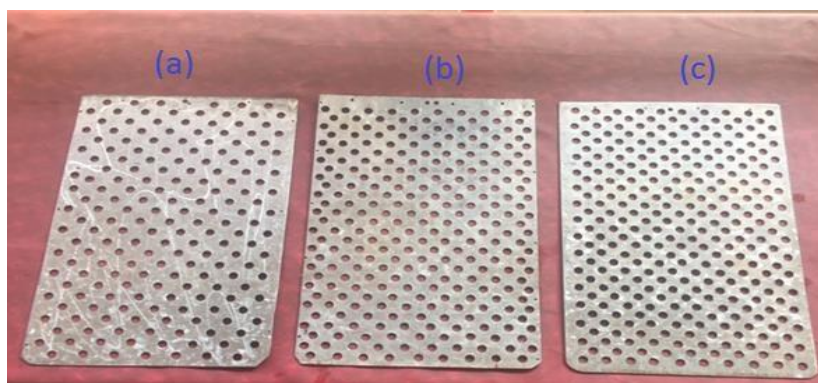

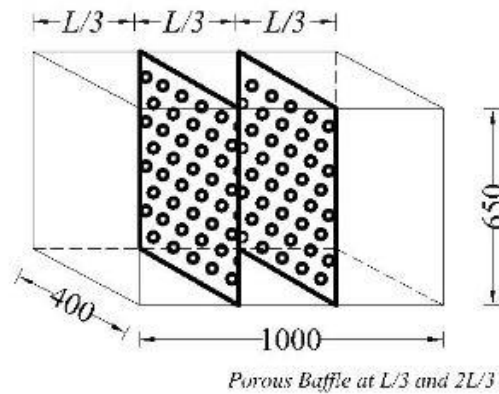Fig. 5 Photographic of porous baffles (a) 15%, (b) 20% and, (c) 25%

Fig. 6 Tank with dual vertical porous baffle (dimensions are in mm)

used for the investigation. In the present study, baffles were placed at *L*/3 and 2*L*/3 location in the rectangular tank. Three different porosities 15%, 20% and 25% porous baffles were used. The staggered pores arrangement is shown in Fig. 4. The fabricated porous baffles are shown in the Fig. 5.

4. Results and discussion

4.1 Free surface elevation

The test was carried out for longer enough to reach a stable state of sloshing. For the altered frequency ratios of 0.163, the surface elevation time histories are shown in Fig. 7. As the frequency ratio increased to $f = f/f_1 = 1$ the oscillation of the free surface elevation is greatly intensified, which is nothing but the first mode of the normal frequency of the fluid, as seen in Fig. 7(a). This is since the energy absorbed by the movement is exceeded as the oscillation of tank coincides with the flow oscillations.

It is observed that when frequency of oscillation and systems normal vibration coincide with each other, the flow continues to consume more energy than the varied one. From Fig. 7(b), when $f = f_2$, i.e., it matches with 2nd mode of natural frequency, the difference in free surface elevation is not high as compared with neighboring frequency ratios. In the case of excitation frequency equal to the second mode normal frequency there is no rapid rise in amplitude of the free surface elevation. Fig. 7(b) illustrates weak sloshing for f_2 frequency ratio.

In this scenario, some of the fluids oscillation capacity will be absorbed by the opposing force caused by the fluctuation in the tank. The rate of sloshing is affected by the frequency of excitation over a variation similar to normal frequencies as the frequency rises from f_2.

Thus, with comparison to nearby frequency ratio the free surface elevations are amplified at $f3$, $f4$ and $f5$ as observed in Figs. 7(c), 7(d) and 7(e), respectively. Based on the findings, for free surface elevations for various frequency ratios, we can conclude that in all three water depth cases, the resonant frequency is precisely the primary mode of the natural frequency of the considered fluid.
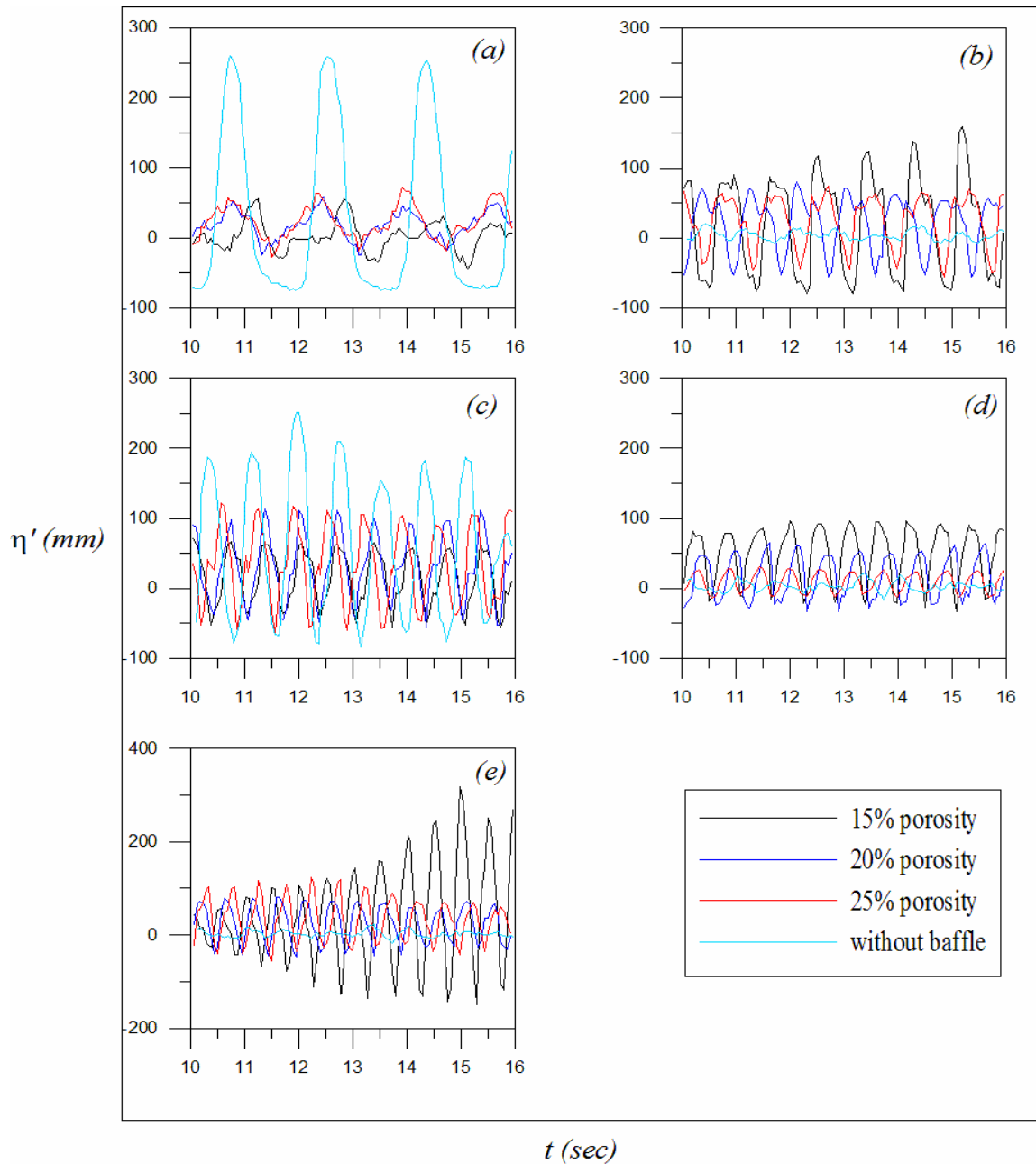
Fig. 7 Time histories of free surface elevation response for $h_s/L = 0.163$, (a) $f = 0.6059\ Hz\ (f_1)$, (b) $f = 1.0967\ Hz\ (f_2)$, (c) $f = 1.4604\ Hz\ (f_3)$, (d) $f = 1.7276\ Hz\ (f_4)$ and, (e) $f = 1.9637\ Hz\ (f_5)$

Similar trend of results have been obtained for the aspect ratios of 0.325 and 0.488 which are projected in Figs. 8 and 9 respectively.
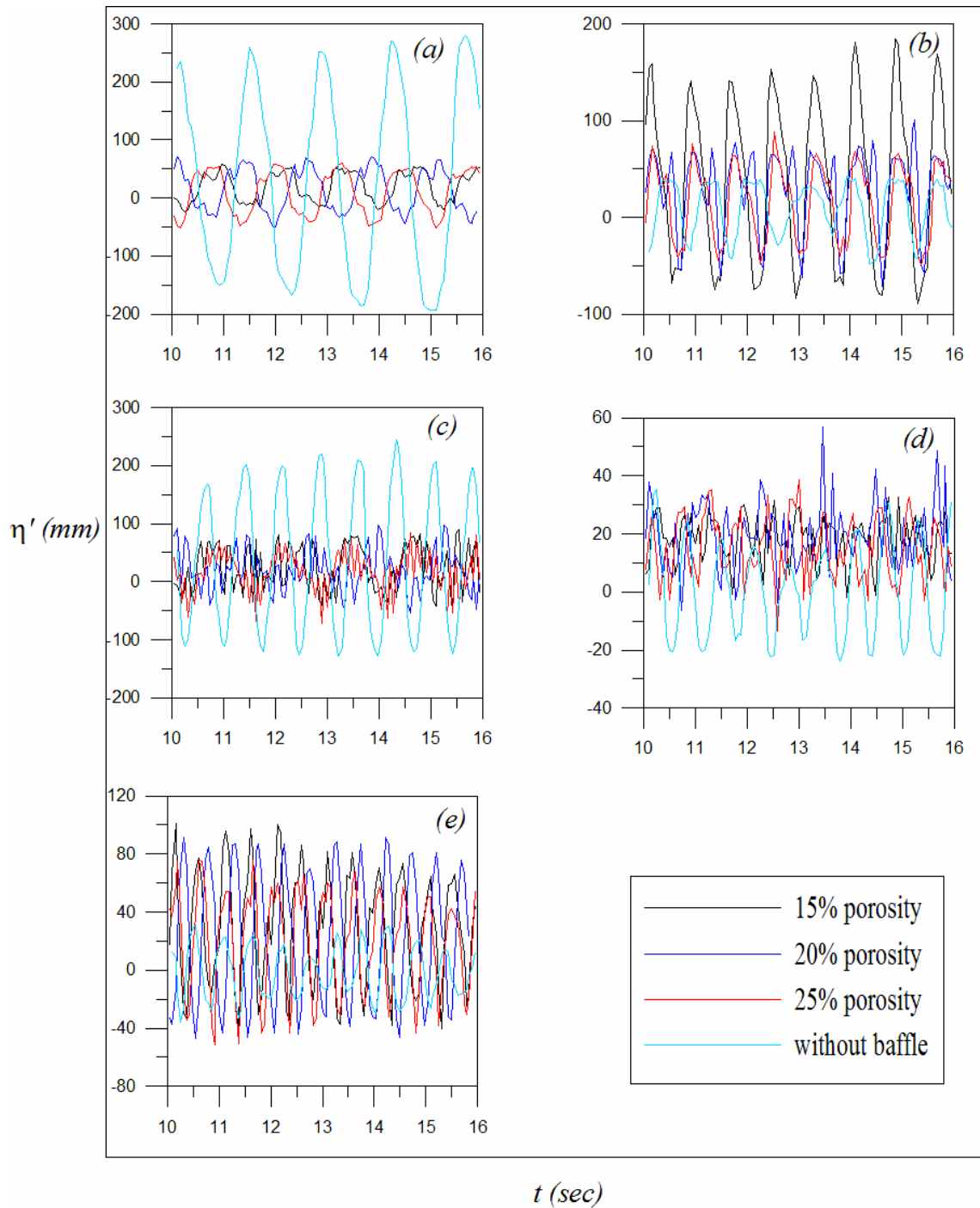
Fig. 8 Time histories free surface elevation response for $h_s/L = 0.325$, (a) $f = 0.7755$ *Hz* (f_1), (b) $f = 1.2287$ *Hz* (f_2), (c) $f = 1.4604$ *Hz* (f_3), (d) $f = 1.7276$ *Hz* (f_4) and, (e) $f = 1.9637$ *Hz* (f_5)
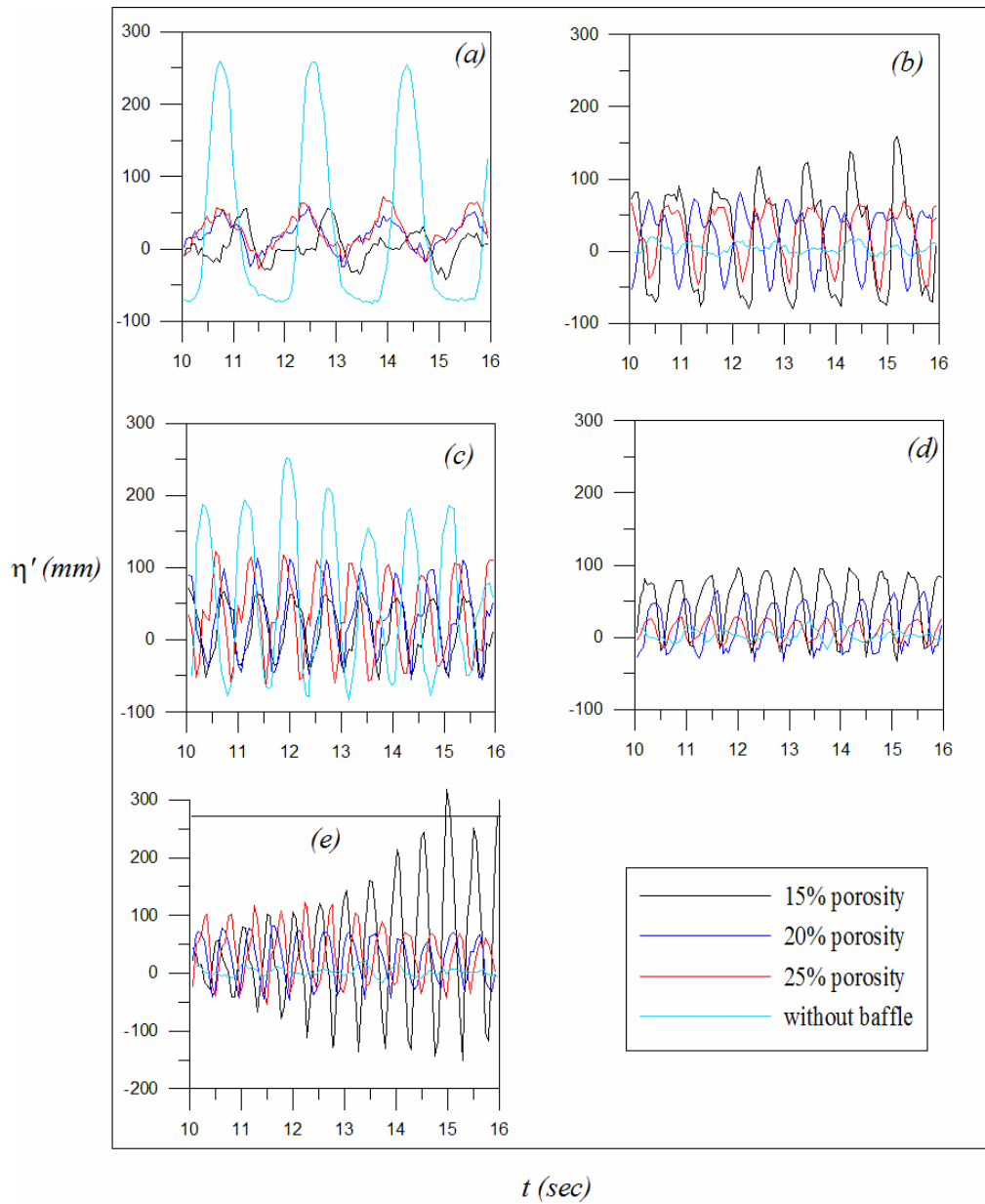
Fig. 9 Time histories free surface elevation response for $h_s/L = 0.488$, (a) $f = 0.8432$ *Hz* (f_1), (b) $f = 1.2468$ *Hz* (f_2), (c) $f = 1.5302$ Hz (f_3), (d) $f = 1.7671$ *Hz* (f_4) and, (e) $f = 1.9757$ *Hz* (f_5)

4.2 Energy dissipation

The frequency dependent energy dissipation characteristics of fluid may be described the response of the dampers to an imposed harmonic displacement. Energy dissipation due to baffle screen is measured by the liquid sloshing fluctuation inside the tank. Energy dissipation is the ratio

of spilling wave energy measured at any particular location with any dampening system inside the tank to energy measured during the absence of dampening system inside the sloshing tank. Graphs are plotted against normalized energy and frequency ratios.

$$E_w^{'} = \frac{Ed}{\frac{1}{2} m_w (2\pi fA)^2} \tag{2}$$

Where, A is the excitation amplitude, m_w is the total mass of the fluid and f is the excitation frequency. Ed is the energy dissipated and E'_w is normalized energy.

- From the above graphs figs. 10-12, the following are observed. As the fill level increases normalized energy decreases for with and without porous baffle condition. For without baffle condition, first and fifth sloshing modes energy is high. At the excitation frequencies of first and fifth sloshing modes energy decreases as increasing the porosity of baffles.
- For third mode excitation frequency, energy dissipation increases with increasing the porosity of baffles. The energy dissipation for 25% fill level is more as compared with 50% fill level and 75% fill level.
- As the fill level increases normalized energy decreases for with and without porous baffle condition.
- For without baffle condition, first and fifth sloshing modes energy dissipation is higher
- At the excitation frequencies of first and fifth sloshing modes energy decreases as increasing the porosity of baffles.
- For third mode excitation frequency, energy dissipation increases with increasing the porosity of baffles.
- When the harmonic input is precisely tuned to the sloshing frequency, the optimal energy dissipation does not occur according to the results of the experiments performed under harmonic motion.
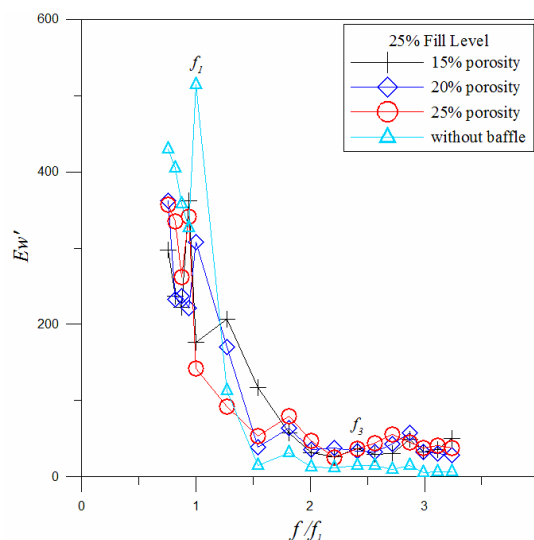

Fig. 10 Dimensionless dissipated energy for excitation amplitude of 7.5 mm with and without porous baffles for $h_S /L = 0.163$
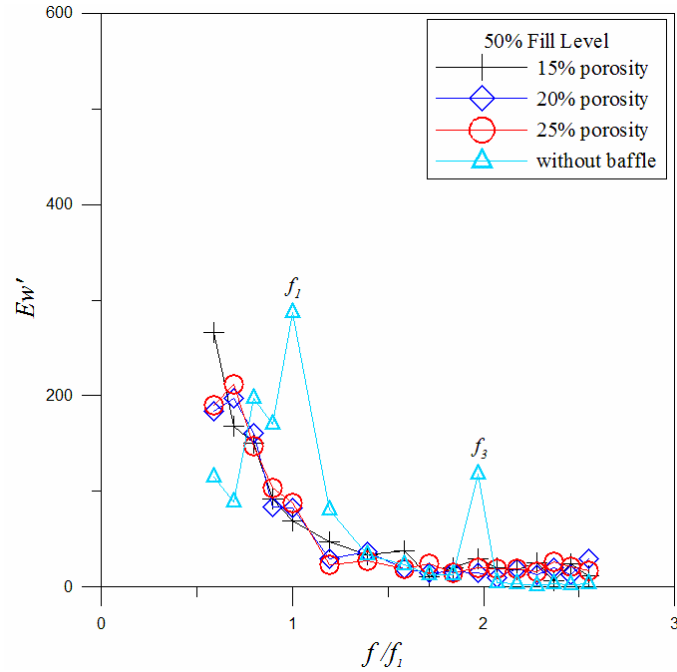
Fig. 11 Dimensionless dissipated energy for excitation amplitude of 7.5 mm with and without porous baffles for $h_S/L = 0.325$
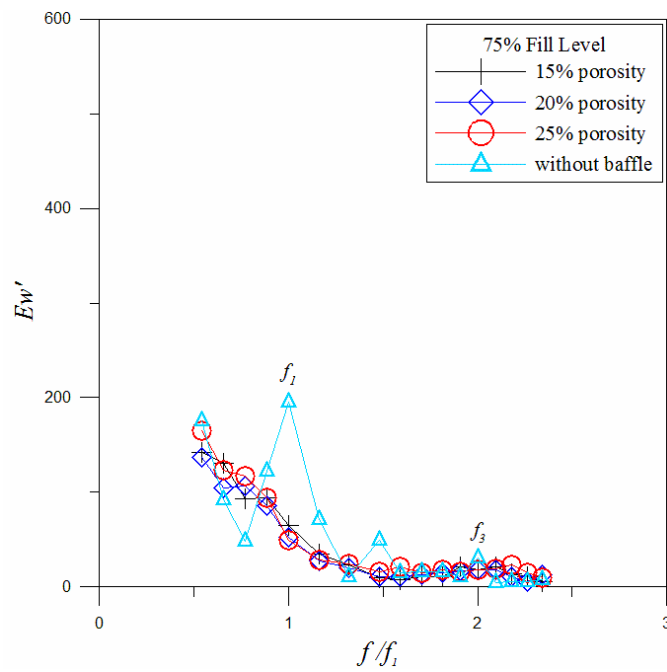

Fig. 12 Dimensionless dissipated energy for excitation amplitude of 7.5 mm with and without porous baffles for $h_S/L = 0.488$

4.3 Sloshing force time series

Force due to the participating fluid is called as sloshing force. The portion of the fluid that generates the dynamic sloshing force is called as participating fluid. Sloshing forces are significant in design of containment walls of partially filled excited tanks and structural integrity with the main structure. Fig. 13 represents the temporal evolution of sloshing force for the excitation amplitude of 7.5 mm. Sloshing force time histories for 25%, 50% and 75% fill levels at $L/3$ and $2L/3$ to the scaled rectangular tanks (i.e., 1:43) with an excitation at odd mode sloshing frequencies (i.e. $f_1, f_3,$ and f_5) are discussed within.
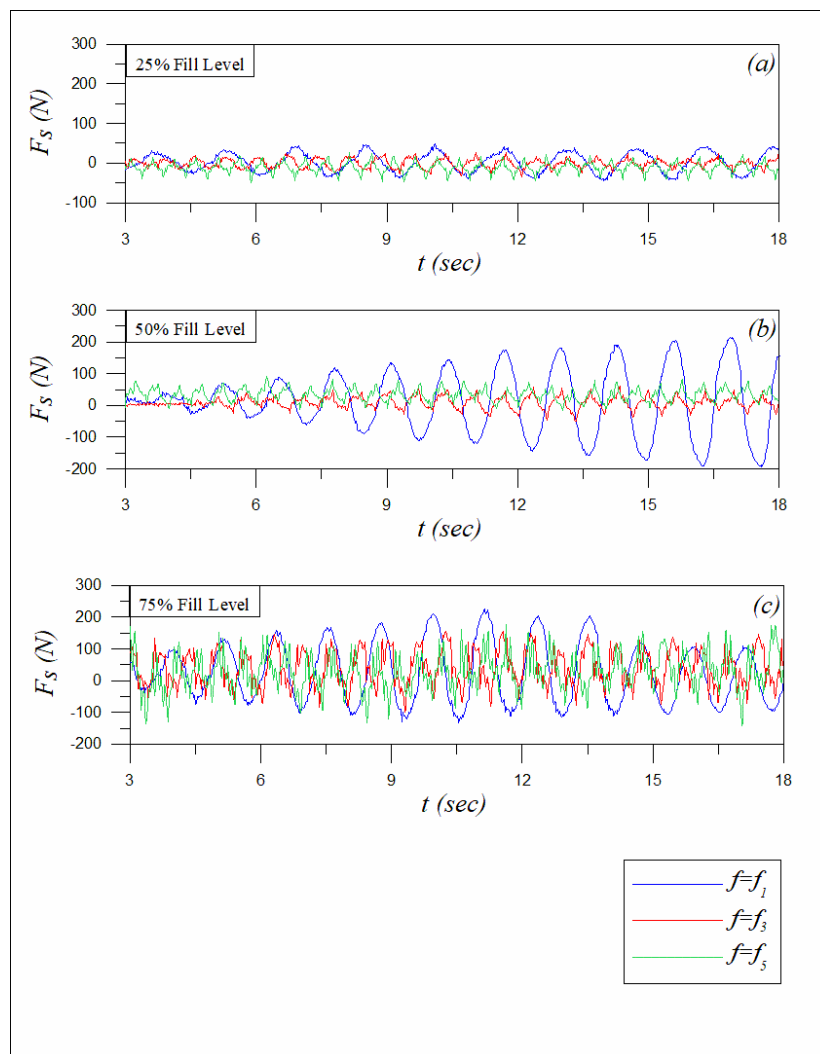

Fig. 13 Time histories of sloshing force corresponding to excitation amplitude for without baffle $h_s/L = 0.163$ (a) $f = 0.6059\ Hz\ (f_1), f = 1.4604\ Hz\ (f_3), f = 1.9637\ Hz\ (f_5), h_s/L = 0.325$, (b) $f = 0.7755\ Hz\ (f_1), f = 1.5270\ Hz\ (f_3), f = 1.9757\ Hz\ (f_5)$, and $h_s/L = 0.488$ and (c) $f = 0.8432\ Hz\ (f_1), f = 1.5302\ Hz\ (f_3), f = 1.9757\ Hz\ (f_5)$
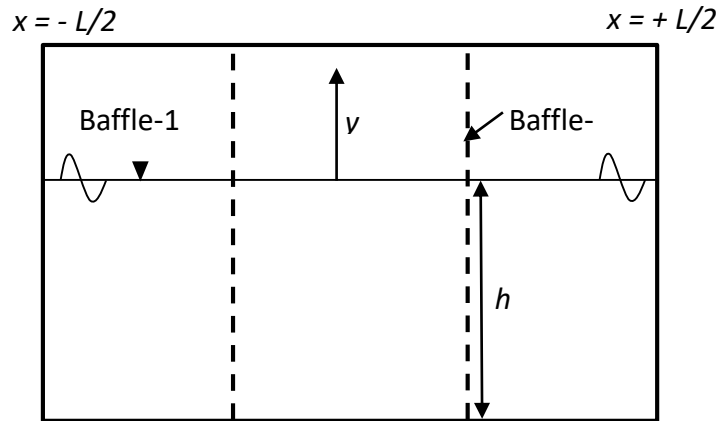
Fig. 14 Schematic diagram of a dual vertical porous baffle

Comparison of the time histories of sloshing force leads to the following observations:

- It is evident that $f = f_1$ is the critical mode of sloshing frequency. It's because, regardless of the fill levels or excitation amplitudes, the largest sloshing force is seen at $f = f_1$.
- The decreasing order of sloshing force is at $f = f_1, f = f_3$ and at $f = f_5$ mode sloshing frequencies irrespective of the fill levels and excitation amplitudes.
- As the excitation amplitude increases, sloshing force also increases irrespective of the fill levels.
- As seen from graphs, sloshing forces are maximum at 50% fill level in comparison with 25% and 75% fill levels.

5. Numerical work

Under the framework of small-amplitude two-dimensional water wave theory, the sloshing responses of the fluid mass in a partially filled swaying rectangular tank with a pair of thin vertical porous baffles extending along the tank height are investigated. The vertical porous barriers are evenly distributed across the tank's center. The porous baffles are numbered sequentially from leftward to rightward.

In the Cartesian coordinate system, the x- axis is taken along the horizontal axis and y- axis is vertically positive upward with the origin $(0, 0)$ chosen at the mean free surface as shown in Fig. 14. The watery is believed to be incompressible and inviscid, and simple harmonic in time with angular frequency ω (Vijay et.al 2020). Hence, there exists a velocity potential $\Phi(x,y,t)$ of the form $\Phi(x,y,t) = \text{Re}\{\phi(x,y)e^{-i\omega t}\}$, where Re denotes the complex potential $\phi(x,y)$ that satisfies the Laplace equation

$$\frac{\partial^2 \phi}{\partial x^2} + \frac{\partial^2 \phi}{\partial y^2} = 0. \tag{3}$$

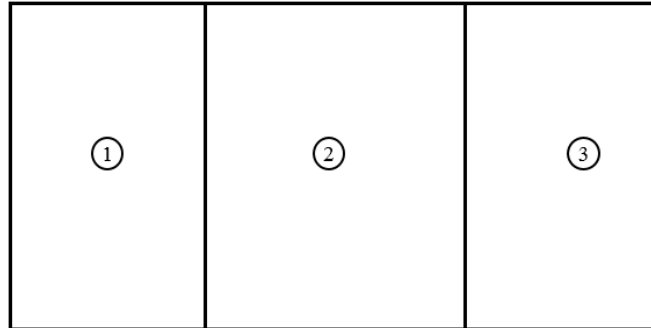On the mean free surface, the linearized boundary condition is given by

Fig. 15 Computation domain of a dual vertical porous baffles

$$\frac{\partial \phi}{\partial y} - \frac{\omega^2}{g}\phi = 0, \quad \text{on} \quad y = 0, \quad -a < x < a. \tag{4}$$

The uniform rigid bottom boundary condition is given by

$$\frac{\partial \phi}{\partial y} = 0, \quad -a < x < a \text{ and } y = -h. \tag{5}$$

The boundary condition on the vertical walls is given by

$$\frac{\partial \phi}{\partial y} = -i\omega n_x, \quad x = \pm a \text{ and } -h < y < 0. \tag{6}$$

The movement past baffle is believed to follow Darcy's law, with the flow being caused by a linear pressure drop through the barrier. The boundary condition on the porous baffle is known by (Cho and Kim 2016).

$$\frac{\partial \phi^-}{\partial x} = -\frac{\partial \phi^+}{\partial x} = i\sigma\left(\phi^- - \phi^+\right) - i\omega n_x. \tag{7}$$

The superscripts $^-$ and $^+$ denote the region before and after the porous baffle respectively. The swaying motion of the tank, which is considered in the second term of the above equation influences the standard velocity of the fluid flow as the tank is horizontally excited. The permeable effect parameter σ denotes the dissipation of energy caused by the baffle for the fluid flow without accounting for the effects of wave breaking. Based on experiments, an empirical relation for the porosity and the porous effect parameter given by (Cho and Kim 2008) is

$$\sigma = \frac{bk}{2\pi} \quad \text{where } b = 57.63P - 0.9717, \ 0.05 \le P \le 0.40 \tag{8}$$

5.1 Numerical solution using BEM

$$\beta^j\left(x_0, y_0\right)\phi^j\left(x_0, y_0\right) = \int_{\Gamma^j} \left(\begin{array}{c} \phi^j\left(x, y\right)\dfrac{\partial G^j\left(x, y; x_0, y_0\right)}{\partial n^j} \\ -G^j\left(x, y; x_0, y_0\right)\dfrac{\partial \phi^j\left(x, y\right)}{\partial n^j} \end{array} \right) d\Gamma^j\left(x, y\right) \tag{9}$$

Where $j = 1, 2, 3$ are the computational domain under consideration. The free term coefficient $\beta^j(x_0, y_0)$ is given by

$$\beta^j(x_0, y_0) = \begin{cases} 1 & (x_0, y_0) \in \Omega, \\ 0.5 & (x_0, y_0) \in \Gamma, \\ 0 & (x_0, y_0) \notin \Omega \cup \Gamma. \end{cases} \tag{10}$$

The ultimate result [22] G^j (also known as free-space Green's function) and derivative $\partial G^j / \partial n^j$ corresponding to the Laplace equation in two-dimensions are given by

$$G^j = \frac{1}{2\pi} \ln r; \quad \frac{\partial G^j}{\partial n^j} = \frac{1}{2\pi r} \frac{\partial r}{\partial n} \tag{11}$$

Where r is the field point distance (x, y) and the source point (x_0, y_0) and is given as

$$r = \sqrt{(x - x_0)^2 + (y - y_0)^2}. \tag{12}$$

It must be observed that for irregular geometry, determining the integral equation's empirical solution in Eq. (9) is extremely difficult, so some kind of mathematical approximation would be relevant. The of each region's domain boundaries are simulated into N^j constant components. Over each component, assume that the velocity potential and its common derivate are constant. Using Eqs. (3)-(8) and the discretized form at the mid-point of each variable, a system of linear algebraic equations

is obtained

$$\sum_{p=1}^{N^j} \sum_{q=1}^{N^j} \frac{\partial \phi_q^j(x, y)}{\partial n^j} \left[\int_{\Gamma_q^j} G_q^j(x, y; x_0, y_0) d\Gamma_q^j(x, y) \right]$$

$$= \sum_{p=1}^{N^j} \sum_{q=1}^{N^j} \phi_q^j(x, y) \left[\int_{\Gamma_q^j} \frac{\partial G_q^j(x, y; x_0, y_0)}{\partial n^j} d\Gamma_q^j(x, y) - \alpha_q^j(x_0, y_0) \right] \tag{13}$$

The domain is denoted by the superscripts, while the domain's boundary element is marked by the subscripts. In order to calculate the boundary integrals in Eq. (13), we adopt the analytical expressions derived by Kelmanson (1983). As associated to the mathematical gauss quadrature process, the main benefit of using analytical expressions for these integrals is the significant time savings. Applying the boundary conditions given in before section in Eq. (13) gives rise to a set of algebraic equations. We solve that to get the unknown potentials for each discrete boundary element. Once the potentials are obtained, the maximum surface wave elevation at the tank walls are computed using

$$\eta_{\max} = \left| \frac{-i\omega\phi}{g} \right|, \quad x = \pm a \text{ and } y = 0. \tag{14}$$

5.2 Maximum free surface oscillation

Figs. 16 and 17 shows the observation of the numerical analysis with the experimental results as a function of non-dimensional excitation frequency. It can be shown that the empirical results in all
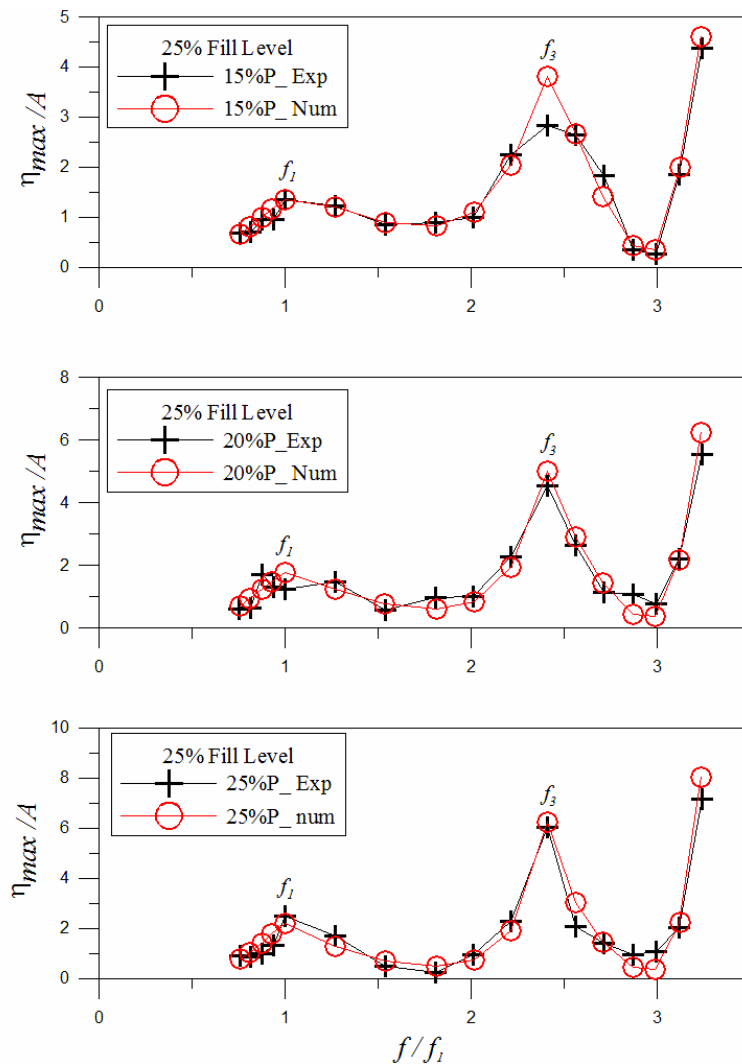
Fig. 16 Variation of $\eta_{\max}$ / A with different porous baffles for three porosities with various frequencies ratio for $h_s/L = 0.163$

the plots indicate an over prediction. This is due to the linearized numerical model assumed. In the potential flow theory, the flow is called inviscid. In experiment details, during the fluid transition through the pores of the baffle, an amount of energy is dissipated. Though Cho *et al.* (2017)'s empirical relationship can be taken into account to some degree, there are other losses, such as flow separation near the tank walls and nonlinearity associated with it. As the ratio of frequency of excitation increases, the bandwidth of the frequencies and their non-dimensional amplitude decreases and increases respectively.

Comparing with porous baffles of $h_s/L = 0.163$ for all three porosities, maximum free surface response elevation decreases for the excitation at first sloshing mode and increases for third sloshing mode frequencies. The free surface elevation increases with increasing the porosities (0.25) for
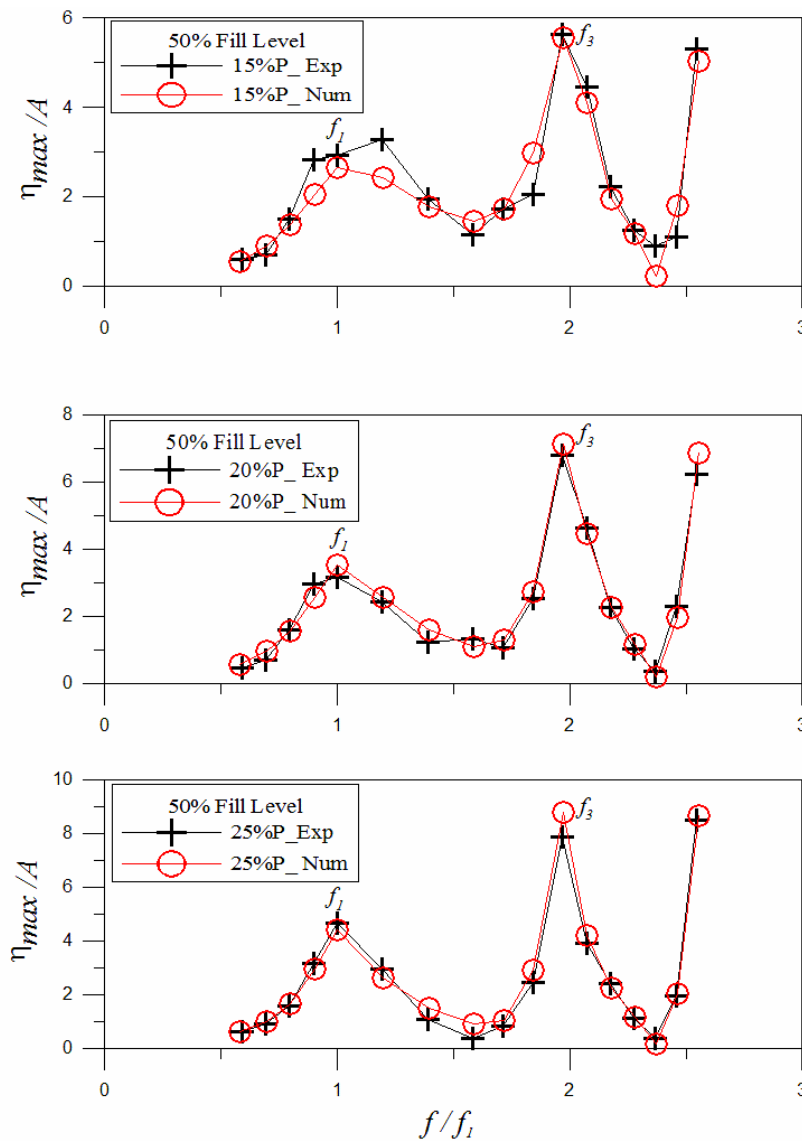
Fig. 17 Variation of η_{max} / A with different porous baffles for three porosities with various frequencies ratio for *hs/l*= 0.325

excitation frequencies considered. Maximum sloshing response is observed at $f = f_3$ both experiment and BEM for the porous conditions rather at $f = f_1$. By considering with baffle condition higher response are observed in the order of $f = f_1$, $f = f_3$ i.e., at odd mode sloshing frequencies. Maximum sloshing response at $f = f_1$ is completely suppressed by all porous baffle conditions. Sloshing response is observed to be increased at $f = f_3$ and slightly decreased due to the presence of porous baffle both experimentally and numerically.

Experimental results of porous conditions are compared with numerical work. It can be seen that a better correlation and maximum response at $f = f_1$ and $f = f_3$ is predicted exactly.

6. Conclusions

The dynamics of liquid sloshing with the assistance of a shake table facility is investigated. Sloshing in liquid tank is sensitive to water deepness. The first mode natural frequency according to the spectrum, has a dominant function and corresponds to a high power density. For with and without baffle conditions, the results showed that aspect ratio of 0.163 gives better free surface elevation and energy dissipation than obtained for aspect ratio 0.325 and 0.488.

The sloshing together with ship motion problem is known to be highly frequency sensitive. The sloshing becomes nonlinear when excitation reaches natural frequency, likely to require detailed calculation on nonlinear sloshing. As the dimensions of the sloshing tank increases or scaling decreases, the number of peak responses, i.e. number of harmonics in the sloshing energy spectrum decreases. The obtained results show that the spectral response of the fundamental liquid sloshing natural frequency is the most important factor in free surface vertical displacement.

Acknowledgments

References

Akyildiz, H. and Ünal, E. (2005), "Experimental investigation of pressure distribution on a rectangular tank due to the liquid sloshing", *Ocean Eng*., **32**(11-12), 1503-1516.
Armenio, V. and La Rocca, M. (1996), "On the analysis of sloshing of water in rectangular containers: Numerical study and experimental validation", *Ocean Eng*., **23**(8), 705-739.
Biswal, K.C., Bhattacharyya, S.K. and Sinha, P.K. (2004), "Dynamic response analysis of a liquid-filled cylindrical tank with annular baffle", *J. Sound Vib.*, **274**(1-2), 13-37.
Cho, I.H. and Kim, M.H. (2008), "Wave absorbing system using inclined perforated plates", *J. fluid Mech*., **608**, 1.
Cho, I.H. and Kim, M.H. (2016), "Effect of dual vertical porous baffles on sloshing reduction in a swaying rectangular tank", *Ocean Eng*., **126**, 364-373.
Cho, I.H., Choi, J.S. and Kim, M.H. (2017), "Sloshing reduction in a swaying rectangular tank by an horizontal porous baffle", *Ocean Eng*., **138**, 23-34.
Cho, I.L.H. (2015), "Sloshing analysis in rectangular tank with porous baffle", *J. Ocean Eng. Tech*., **29**(1), 1-8.
Frandsen, J.B. (2004), "Sloshing in excited tanks", *J. Comp. Phys*., **196**, 53-87.
Goudarzi, M.A. and Sabbagh-Yazdi, S.R. (2012), "Investigation of nonlinear sloshing effects in seismically excited tanks", *Soil Dynam. Earthq. Eng*., **43**, 355-365.
Ibrahim, R.A. (2005), "Liquid Sloshing Dynamics", Theory and Applications. *Cambridge University Press*, New York.
Isaacson, M. and Premasiri, S. (2001), "Hydrodynamic damping due to baffles in a rectangular tank", *Can. J. Civil Eng.*, **28**(4), 608-616.
Jiang, M., Bing, R., Wang, G. and Wang, Y. (2014), "Laboratory investigation of the hydroelastic effect on liquid sloshing in rectangular tanks", *J. Hydrodynam.*, **26**(5), 751-761.
Jin, H., Liu, Y., Li, H. and Fu, Q. (2017), "Numerical analysis of the flow field in a sloshing tank with a horizontal perforated plate", *J. Ocean Univ. China*, **16**(4), 575-584.

Kang, H.S., Md Arif, U.G., Kim, K.S., Kim, M.H., Liu, Y.J., Lee, K.Q. and Wu, Y.T. (2019), "Sloshing suppression by floating baffle", *Ocean Syst Eng*., **9**(4), 409-422.

Kelmanson, M.A. (1983), "Boundary integral equation solution of viscous flows with free surfaces", *J. Eng. Math*., **17**(4), 329-343.

Kim, S., Kim, Y. and Lee, J. (2017), "Comparison of sloshing-induced pressure in different scale tanks", *Ships Offshore Struct*., **12**(2), 244-261.

Nakayama, T., and Washizu, K. (1980), "Nonlinear analysis of liquid motion in a container subjected to forced pitching oscillation", *Int. J. Numerical. Method. Eng*., **15**, 1207–1220.

Nasar, T., and Sannasiraj, S. A. (2019), "Sloshing dynamics and performance of porous baffle arrangements in a barge carrying liquid tank", *Ocean Eng*., **183**, 24-39.

Nasar, T., Sannasiraj, S.A. and Sundar, V. (2012), "Liquid sloshing dynamics in a barge carrying container subjected to random wave excitation", *J. Nav. Archit. Mar. Eng*., **9**(1), 43-65.

Poguluri, S.K., Kim, J., George, A. and Cho, I.H. (2021), "Experimental and numerical investigation of a surface-fixed horizontal porous wave barrier", *Ocean Syst. Eng*., **11**(1), 1-16.

Vijay, K.G., Neelamani, S., Sahoo, T., Al-Salem, K. and Nishad, C.S. (2020), "Scattering of gravity waves by a pontoon type breakwater with a series of pervious and impervious skirt walls", *Ships Offshore Struct*., 1-13.

Xue, M.A., Zheng, J., Lin, P. and Yuan, X. (2017), "Experimental study on vertical baffles of different configurations in suppressing sloshing pressure", *Ocean Eng*., **136**, 178-189.

Yu, L., Xue, M.A. and Zheng, J. (2019), "Experimental study of vertical slat screens effects on reducing shallow water sloshing in a tank under horizontal excitation with a wide frequency range", *Ocean Eng*., **173**, 131-141.

MK